

The PAMELA Calorimeter Identification Capabilities

J. Lundquist^a, J. Lund^b, M. Boezio^a, V. Bonvicini^a, E. Mocchiutti^a, M. Pearce^b,
P. Schiavon^a, A. Vacchi^a, F. Volpe^c, G. Zampa^a and N. Zampa^a

(a) INFN, Structure of Trieste and Physics department of University of Trieste, Via Valerio 2, I - 34127 Trieste, Italy

(b) The Royal Institute of Technology(KTH), Dept. of Physics, Albanova University Centre, SE-10691, Stockholm, Sweden

(c) INFN, Structure of Bari and Physics Department of University of Bari, Via E. Orabona 4, I - 70126 Bari, Italy

Presenter: J. Lundquist (lundq@ts.infn.it), ita-lundquist-J-abs1-og15-oral

A silicon-tungsten imaging calorimeter has been designed, built and successfully integrated in the PAMELA satellite-borne apparatus. The main physics task of the experiment is the measurement of the flux of antiprotons, positrons and light nuclei in the cosmic radiation. The purpose of the calorimeter is to separate antiprotons and positrons from the vast background of cosmic-ray electrons and protons, respectively. In this work we present the identification capabilities of the calorimeter obtained using both Monte Carlo and test beam data. We show that the calorimeter can provide a proton rejection factor of about 10^5 while keeping a $\sim 90\%$ efficiency in selecting electrons and positrons. The PAMELA calorimeter is therefore able to provide the identification power needed to reach the primary scientific objectives of PAMELA.

1. Introduction

PAMELA [1] is a satellite-borne experiment primarily designed to measure the properties of antimatter in the cosmic radiation. The apparatus consists of a permanent magnet/silicon tracker, a silicon-tungsten imaging calorimeter, a time-of-flight (ToF) system, an anticoincidence veto shield, a shower tail catcher scintillator and a neutron detector. PAMELA will be carried by the Resource-DK1 semi-polar orbiting satellite. The planned launch date is at the end of 2005.

The main scientific goal of the experiment is the precise measurement of the cosmic-ray antiproton and positron energy spectra [2]. The substantial backgrounds of protons (for positrons) and electrons (for antiprotons) however complicates the measurements. The ability of the calorimeter to separate electrons from hadrons has been studied by using test beam data and comparisons with simulations.

The PAMELA sampling calorimeter [3] is made of 44 silicon sensor planes interleaved with 22 planes of tungsten absorbers, for a total depth of $16.3 X_0$ (radiation lengths) or 0.6λ (interaction lengths). Each silicon plane is composed of a square matrix of 3×3 detectors. These are large area devices ($8 \times 8 \text{ cm}^2$), each of them is segmented into 32 large strips with a pitch of 2.4 mm and a thickness of $380 \mu\text{m}$. Each of the 32 strips of a detector is wire-bonded to the corresponding one of the other two detectors in the same row (or column), thus forming 24 cm-long strips. The orientation of the strips of two consecutive layers is shifted by 90° , so to have two-dimensional read out.

2. Electron-Hadron Separation

Clean identification of antiprotons and positrons in the cosmic radiation implies high identification capabilities.

The PAMELA Time-of-Flight system can with extremely high accuracy select down-going $|Z| = 1$ particles, and the tracking system provides reliable information on the sign of charge and rigidity (momentum/charge) over a wide range of momenta from about 50 MeV/c up to several hundreds GeV/c. Thus, since PAMELA is a satellite-borne experiment, it remains to identify positrons from a background of protons that increases from

about 10^3 times the e^+ component at 1 GeV/c to about 5×10^3 at 10 GeV/c and antiprotons from a background of e^- that decreases from about 10^3 times the \bar{p} component at 1 GeV/c to less than 10^2 above 10 GeV/c. This means that the PAMELA detectors have to separate electromagnetic from hadronic particles at a level of 10^5 - 10^6 . Most of this identification is provided by the PAMELA calorimeter.

Electromagnetic and hadronic showers differ in their spatial development and energy distribution in a way that can be distinguished by the calorimeter. One difference between an electromagnetic and hadronic cascade is that only for the electromagnetic shower the shower maximum is contained inside the calorimeter for the energy range of interest. Another is that the lateral distribution of the hadronic shower is much wider. Also, the development of the electromagnetic cascade is strongly related to the energy of the primary electron and the electromagnetic shower will with high probability start to develop in the first two to three planes of the calorimeter. For electrons there is a linear relationship between the primary particle energy and the deposited energy (up to ~ 1 TeV for the PAMELA calorimeter).

The variables characteristics of an electromagnetic shower which have been exploited to separate it from a hadronic shower are: the starting point of the shower, the detectable energy loss, the longitudinal profile, the transverse profile and the topological development of the shower.

3. Test Beam and Simulation

The calorimeter hadron/electron separation has been studied using test beam data and simulations. There are two aims to this study. The first is to estimate the calorimeter's rejection capability and electron selection efficiency. The second is a comparison between test beam and simulation which can be used to validate simulation studies of the calorimeter in situations resembling those expected in orbit.

The test beam data used in the analysis were collected at three different occasions at CERN during 2002-2003 both at PS and SPS beam facilities. In none of these tests the calorimeter was in its final configuration (e.g. equipped with half of the silicon planes in 2002 SPS test beam [4]).

The simulations have been performed using variations of the PAMELA Collaboration's official simulation program: GPAMELA [5]. It is based on the GEANT package [6] version 3.21 and uses as default the GHEISHA [7] hadron shower Monte Carlo to simulate the interactions of hadrons with the nuclei of the matter traversed.

4. Results and Conclusions

Several types of variables characterizing an electromagnetic shower have been combined in different ways and with different conditions depending on the test beam and momentum used, and then applied to both the test beam and the simulated data. As an example the energy deposition (for 200 GeV/c e^- and p) in one quarter of the calorimeter is shown in figure 1. A clear separation between the two types of particles can be seen. The arrow indicates the condition used to reject protons.

Figure 2 shows the efficiency (top) and contamination (bottom) of the final electron/positron selection as a function of particle momentum. The full circles represent test beam data and the open squares simulated data. During the analysis, one aim was to keep the electron efficiency at about 90% if possible. As can be seen in the figure, the agreement between simulation and experimental data is acceptable.

In the bottom part of figure the proton contamination as function of particle momentum is shown for both test beam data (full circles) as well as for simulated data (open squares). The arrows mark the 68% confidence level when no events survived the selection. The first two data points (at 3 and 10 GeV/c) are for electron/pion

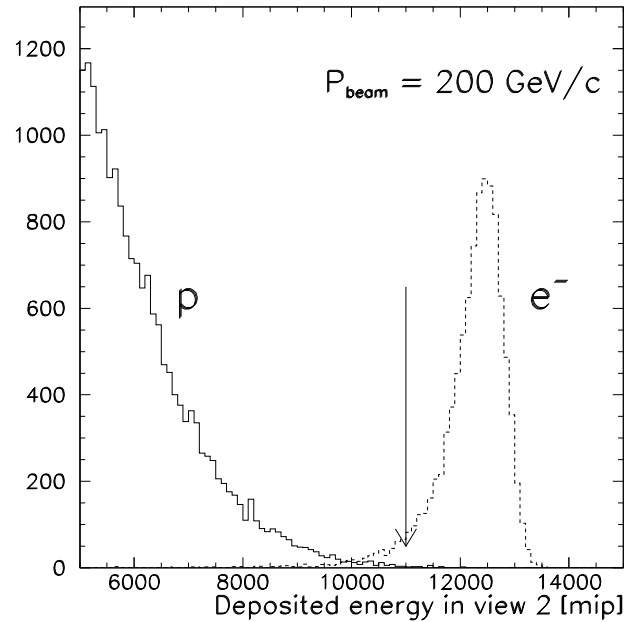


Figure 1. Energy deposited (in mip, most probable energy deposited by a minimum ionizing particle) in one quarter of the PAMELA calorimeter for 200 GeV/c electrons and protons. As the incident particle momentum increases the separation between electrons and protons (here is only showed the high energy tail of the proton distribution) becomes more pronounced, however a tail toward lower deposited energies for the electron distribution (arising from the increased ‘leakage’) can cause a loss in efficiency if a too strict selection is made. The arrow illustrates how this quantity was used to reject protons. About 10^4 e^- and 2.5×10^5 p were collected at this energy.

separation and thus do not directly apply to the electron/proton study. This is because pions of 3 GeV/c momentum have ~ 1 GeV more of kinetic energy that can be deposited in the calorimeter, than protons of the same momentum. This should lead to a higher contamination (worse separation) for pions compared to protons. However, they can be used for comparison between simulation and test beam results and thus the full star and dashed arrow, which mark the results for simulated protons at 3 and 10 GeV/c respectively, should be representative. A good agreement between simulation and test beam data can be seen.

These results refer to a partially equipped calorimeter, hence they can be considered as lower limits of the PAMELA calorimeter performances.

Antiprotons are identified¹ by selecting electromagnetic showers in the calorimeter with the highest possible efficiency and rejecting them. No test beam data are available for antiprotons and only simulation studies were performed (see [3]).

¹At low momenta (below ~ 1.5 GeV/c) \bar{p} are identified also using the velocity measured by the ToF system.

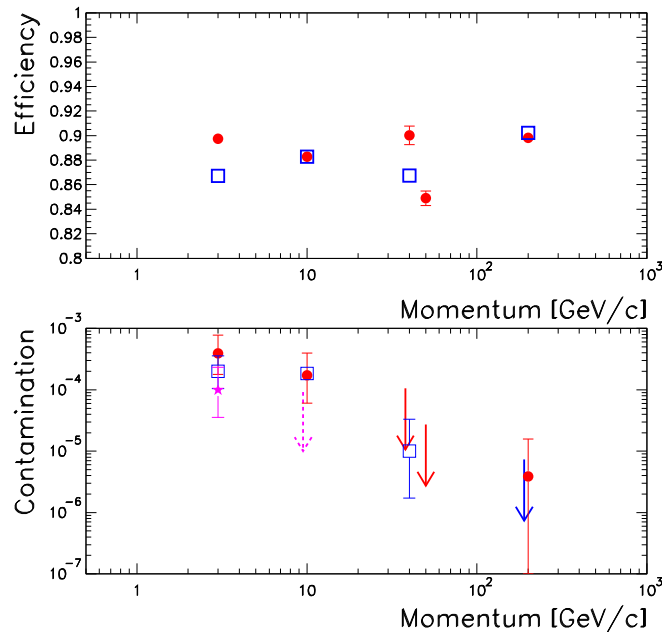


Figure 2. Top: The efficiency for identifying electrons using the electron/positron calorimeter selection as a function of particle momentum. The full circles and open squares represents test beam and simulated data respectively. **Bottom:** The proton contamination of the electron/positron calorimeter selection as a function of particle momentum. The full circles and open squares represent test beam and simulated data respectively, the full triangle is for 3 GeV/c simulated protons, the arrows indicate the 68% confidence level (i.e. no events survived the selection) and the dashed arrow is for simulated protons at 10 GeV/c. The data at 10, 40 and 200 GeV/c are slightly displaced for clarity.

5. Acknowledgments

We thank the PAMELA Collaboration for their support during the test beam measurements and Drs Marialuigia Ambriola and Francesco Cafagna for their help with GPAMELA.

References

- [1] M. Boezio et al., “The Space Experiment PAMELA”, Proceedings of this Conference.
- [2] M. Boezio et al., Nucl. Physics B (Proc. Suppl.) 134, 39 (2004).
- [3] M. Boezio et al., Nucl. Inst. & Meth. A 487, 407 (2002).
- [4] J. Lund, Ph.D. thesis Royal Institute of Technology, Stockholm, (2004). Available at: <http://www.particle.kth.se/>
- [5] <http://www.be.infn.it/ambriola/gpamela>
- [6] R. Brun et al., “Detector Description and Simulation Tool”, CERN program library (1994).
- [7] H. C. Fesefeldt, Technical report PITHA 85-02, Phys. Inst., RWTH Aachen.